Dasaka, S. M. & Zhang, L. M. (2012). *Géotechnique* **62**, No. 5, 375–384 [http://dx.doi.org/10.1680/geot.8.P.151.3786]

Spatial variability of in situ weathered soil

S. M. DASAKA* and L. M. ZHANG†

The founding depths of pile foundations depend primarily on the loading conditions of the superstructure and the strength of subsoil. The depth of Grade III weathered rock, the top of completely decomposed granite (CDG), and standard penetration test *N*-value of 200 (SPT-200) are often used as indicators for decision-making in arriving at the preliminary founding depth of piles in Hong Kong. The work reported in this paper focuses on evaluation of the spatial variability characteristics of the above founding depth indicators at a construction site, using statistical models based on random field theory. Spatial variability characteristics are evaluated using the measured data in terms of scale of fluctuation. Geostatistics is used to obtain additional data at unsampled locations for mapping profiles of founding depth indicators over the site, using the measured data from borehole records and site investigation results. It is observed from the results that, if faults are not present, the depth of the Grade III surface exhibits the largest scale of fluctuation among the three indicators, and the variability of the ground is observed to increase with the weathering grade. The effect of the size of the sampling domain on the autocorrelation characteristics of the founding depth indicators is also studied. The results demonstrate that the scale of fluctuation increases with increase in the size of the sampling domain.

KEYWORDS: geology; piles; residual soils; sampling; site investigation; statistical analysis

La profondeur des fondations sur pieux est tributaire principalement des conditions de charge de la superstructure et de la résistance du sous-sol. On utilise souvent la profondeur de roche altérée de qualité III, le dessus de granit entièrement décomposé, ainsi qu'une valeur d'essai « *N*-value » de 200 à l'essai de pénétration standard (SPT 200), comme indicateurs dans les prises de décision sur la profondeur de pieux de fondation à Hong Kong. Les travaux reportés dans la présente communication se concentrent sur l'évaluation de caractéristiques de variabilité spatiale des indicateurs susmentionnés de profondeur de fondation, sur un chantier de construction, en utilisant des modèles statistiques basés sur la théorie des champs aléatoires. On procède à l'évaluation de caractéristiques de variabilité spatiale, à l'aide de données mesurées sur le plan de l'échelle des fluctuations. On fait usage de géostatistiques afin d'obtenir des données dans des lieux non échantillonnés pour le mappage de profils d'indicateurs de profondeurs de fondations sur le site, en faisant usage des données mesurées d'après les registres de forages et les résultats de reconnaissances sur le site. On relève, dans les résultats, qu'à condition de l'absence de failles, la profondeur de la surface de qualité III est la fluctuation majeure des trois indicateurs, et que la variabilité du sol augmente avec le type d'altération. On se penche également sur l'effet de la taille du domaine d'échantillonnage sur les caractéristiques d'autocorrélation des indicateurs de profondeur de fondation. Les résultats démontrent que l'échelle des fluctuations augmente avec l'augmentation de la taille du domaine d'échantillonnage.

INTRODUCTION

Weathering is a natural and continuous process, in which rocks are subjected to physical, chemical and biological decay, and are transformed to different kinds of materials that are significantly weaker in their properties than the parent materials in the absence of geological faults (Durgin, 1977). The weathering intensity generally decreases with depth as the proportion of rock material increases until the weathering front is reached, where one observes an entirely fresh rock. Considerable variability is associated with the weathered rocks and soil owing to the complex nature of the physical and chemical processes undergone by the parent rock over many years. In most cases the foundations of structures rest on weathered rocks. Accordingly, considerable variability is also encountered in evaluating the geotechnical properties of these supporting strata. Hence the variation in the degree of weathering is very important in the geotechnical characterisation of the supporting strata for foundation design. Neglecting the effects of this variability on foundation performance may eventually lead to an unreliable or costly design.

Geologic features observed in borehole samples provide critical information to assist in the exploration of ground conditions, which is essential for efficient foundation design. The major part of Hong Kong's geology consists of granitic and volcanic rocks of Mesozoic geological age, which are around 100–200 million years old. A detailed description of its geology can be obtained from Fletcher (2004). Hong Kong practice groups the parent rock, weathered rock and soil into six different grades, based on their distinguishing features and the resistance offered by them against certain selected physical tests (GEO, 2000b). For example, Grade IV and Grade V materials, whose classifications are very important for foundation design (Fletcher, 2004), are clearly distinguished by observing whether they slake in water or not. Table 1 shows the complete weathering grade classifications that are adopted in Hong Kong practice.

Pile foundations are generally used to support heavy and tall structures in Hong Kong. In general, the Grade III material is deemed to support the loads of structures effectively by resulting in distortions that are within permissible limits. Hence, for preliminary designs, the depth of Grade III or better rock is often taken as a reference for determining the founding depths of bored piles. Custom and practice

Manuscript received 12 January 2009; revised manuscript accepted 22 September 2011. Published online ahead of print 21 February 2012.
Discussion on this paper closes on 1 October 2012, for further details see p. ii.
* Department of Civil Engineering, Indian Institute of Technology Bombay, Mumbai, India (formerly Department of Civil Engineering, Hong Kong University of Science and Technology).
† Department of Civil and Environmental Engineering, Hong Kong University of Science and Technology.

Table 1. Weathering grades of granites and volcanic rocks and their distinguishing features (after GEO, 2000b)

Decomposition term	Grade symbol	Distinguishing features
Residual soil	VI	No original rock texture preserved; crumbles by finger pressure into constituent grains
Completely decomposed	V	Original rock texture preserved; crumbles by finger pressure into constituent grains; indents easily by point of geological pick; slakes in water; completely discoloured in comparison with fresh rock
Highly decomposed	IV	Original rock texture preserved; breaks into smaller pieces by hand; not easily indented by point of pick; does not slake in water; completely discoloured in comparison with fresh rock
Moderately decomposed	III	Rock completely stained throughout; cannot be broken into smaller pieces by hand; easily broken by geological hammer; makes a dull or slight ringing sound when struck by hammer
Slightly decomposed	II	Fresh rock colours generally retained but stained close to joints; not easily broken by geological hammer; makes a ringing sound when struck by hammer
Fresh	I	No staining; not easily broken by geological hammer; makes a ringing sound when struck by hammer; no visible signs of decomposition (i.e. no discolouration)

further specify that the founding depth of a bored pile should be chosen in such a way that it precedes a continuous 5 m Grade III or stronger material (GEO, 2006). If the Grade III surface is found, but is not continuous for 5 m below this depth, the founding depth would normally be taken to deeper depths where Grade III rock or stiffer material is available for a continuous 5 m.

Figure 1 shows a typical structure of weathered rock, and a simplified profile indicating the different weathering grades for geotechnical design (GEO, 2006). From this figure it is evident that the levels of the top surfaces of different grades of rock across a site may vary considerably.

OBJECTIVES OF THE STUDY

The main objectives of the present study are

(*a*) to map the depths of Grade III weathered rock, top of completely decomposed granite (CDG), and SPT-200 surfaces over a study area in Hong Kong using the measured data from boreholes alone, and both measured data and predicted data at locations where no information is available
(*b*) to evaluate the spatial correlation characteristics of the above parameters using measured data alone, and both measured data and predicted data
(*c*) to identify the effects of the size of the sampling domain on the spatial correlation characteristics of these parameters.

The advantage of getting such information is that it helps engineers to use data derived from nearby sites or sites of similar geological materials subjected to similar geological process to build a preliminary ground model for a new site.

Similar studies have been reported for the evaluation of the spatial characteristics of soil and rock properties for various applications using either geostatistics or random field modelling (Vanmarcke, 1977; Kulatilake, 1989; DeGroot & Baecher, 1993; DeGroot, 1996; Fenton, 1999; Jaksa *et al.*, 1999; Liu & Chen, 2006; Murakami *et al.*, 2006).

For example, DeGroot & Baecher (1993) analysed the spatial correlation of field vane shear strength using a maximum likelihood technique. It was concluded from their study that the estimated spatial correlation characteristics were influenced by sample spacing, with better estimates provided by investigations with a number of borings located at separation distances less than the autocorrelation distance. Fenton (1999) analysed 143 regularly spaced cone tip resistance records, and observed that the scale of fluctuation exhibited sampling domain (size) dependence, in that a larger sampling domain would result in a larger scale of fluctuation.

Jaksa *et al.* (1999), on the other hand, used random field modelling to estimate vertical and horizontal correlation distances of undrained shear strength using cone tip resistance (q_c) data measured at closely spaced regular intervals, and found that they varied in the ranges 60–240 mm and 1–2 m respectively. It was noted that the horizontal spatial

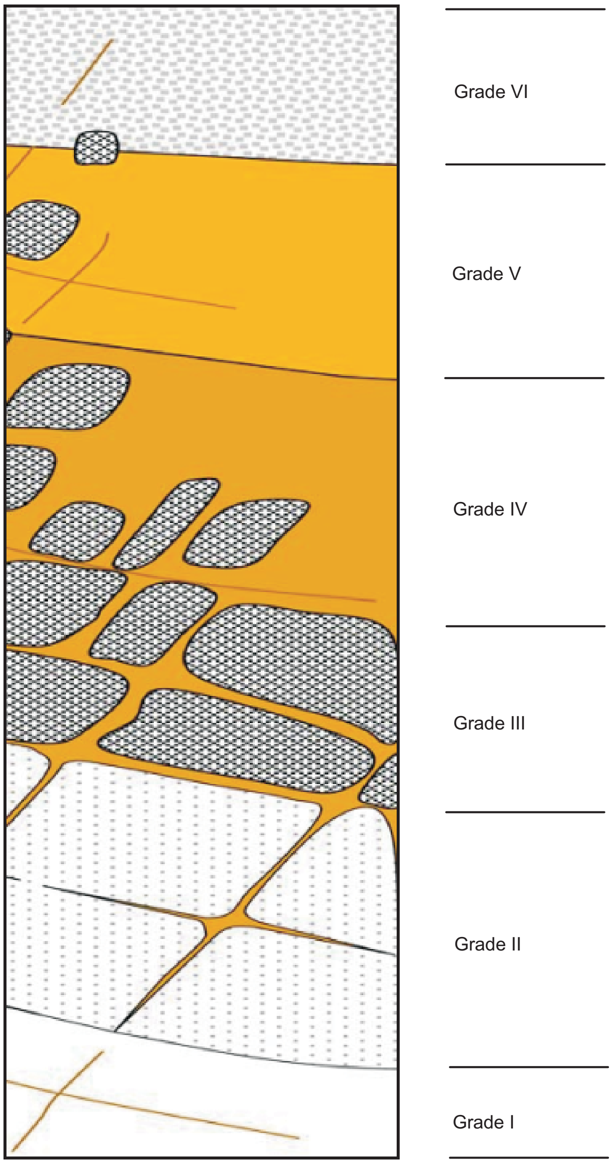

Fig. 1. Typical profile of weathered rock (modified from GEO, 2006)

variability exhibits a nested structure, which means that estimated scales of fluctuation increase with the size of the sampling domain. Liu & Chen (2006) evaluated spatial correlation characteristics of cone tip resistance (q_c) and sleeve friction (f_s) in the horizontal direction to map the liquefaction potential over an extensive area of Yuanlin in Taiwan. In total, 71 profiles of q_c and f_s, spread unevenly across the city, were used in the study. The scales of fluctuation of q_c and f_s were observed to be in the range 100–300 m.

Most of the findings on spatial correlation characteristics available in the literature are based on closely and regularly spaced data in the vertical direction. In the present study, limited in situ measured data in the horizontal direction at irregular spacing, which is common from a routine site investigation programme, are used to achieve the objects delineated above.

STUDY SITE

The borehole data obtained from a site in weathered ground in Hong Kong has been used for this study. The site is rather flat; the ground surface is, on average, at 5·7 m above the mean sea level, and no geological fault is reported at this site. The site is divided into seven blocks for site exploration purposes, which are hereafter referred to as blocks 1 to 7. Table 2 shows the number of boreholes, in which information about Grade III, SPT-200 and CDG profile depths is available, over the whole site, for blocks 1, 2 and 3 combined, and for block 1 alone. The sizes of the exploration area for the whole site, for blocks 1, 2 and 3 together, and for block 1 alone for each profile are given in Table 3. Fig. 2 shows the locations of the boreholes, which are irregularly spaced within the site. Following the Hong Kong practice (GEO, 2000a), some boreholes were sunk to reveal the depth of Grade III weathered rock, top of CDG and the SPT-200 surface in the preliminary site investigation stage on a grid of about 30 m spacing. Subsequently more boreholes were sunk to reveal the depth of Grade III weathered rock at the north-east part of the site, where bored piles were adopted to support three buildings (1, 4 and 6) and one borehole was sunk at every pile location to determine the Grade III rockhead level. Additional boreholes were sunk to support the design of driven H piles for the remaining four buildings (2, 3, 5 and 7), particularly at locations where preboring was needed, or where the variations in the SPT-200 and Grade III rockhead levels were large (Zhang & Dasaka, 2010). These boreholes were terminated as soon as five consecutive SPT-N values higher than

Table 2. **Number of measured data in individual blocks and the whole site**

	Grade III	SPT-200	Top of CDG
Whole site	174	227	228
Blocks 1, 2 and 3 together	87	96	97
Block 1 alone	49	48	49

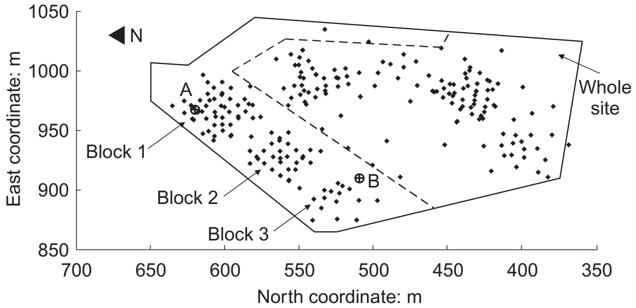

Fig. 2. Plan of borehole locations within the whole site

200 had been encountered. The different kinds of rock and soil layer were identified using physical tests and the information obtained from borehole logs. Standard penetration tests (SPTs) were also conducted at the site to gain additional information. Core stones were encountered at the site, and a small fraction (about 6%) of the SPTs were terminated at various levels in a borehole to protect the SPT shoe. From the reported refusal values, the SPT *N*-values are linearly extrapolated and used in the analysis.

SPATIAL CORRELATION CHARACTERISTICS

To evaluate the spatial variability of a set of data using statistical models based on geostatistics and random field modelling, it is essential that the data are stationary: that is, the statistical properties of the data are not affected by any shift of the spatial origin or, statistically, the first two moments (mean and variance) are required to be constant, a condition termed 'weak' or second-order stationarity. The original measured dataset should be evaluated first. If the dataset is stationary, then analysis can be performed on the data directly. If the dataset is non-stationary, treatment must first be given to transform the data, by which the non-stationary dataset is transformed to a stationary set by removing the deterministic component called the trend, and the stationary residual random component is then analysed.

The trend-removal method has been more widely used in geotechnical literature than other methods of data transformation. This method aims to estimate and remove the trend, and make the residual random component stationary. Stationarity of the data is achieved by removing a low-order polynomial trend of no higher order than quadratic (Lumb, 1974; Brooker, 1991), which is usually estimated by the ordinary least squares (OLS) error approach (Journel & Huijbergts, 1978). In most of the studies, the trend function is simply estimated by regression analysis using either linear or polynomial curve fittings (Campanella *et al.*, 1987; Kulhawy *et al.*, 1992).

Geostatistics

Geostatistics was initially developed to assist in the estimation of changes in ore grade within a mine. Owing to the successful application of geostatistics principles in mining engineering, its application has been made use of in diversi-

Table 3. Size of exploration area for individual blocks and the whole site

	Grade III	SPT-200	Top of CDG
Whole site	160·2 m × 252·4 m	160·2 m × 266·3 m	160·2 m × 266·3 m
Blocks 1, 2 and 3 together	122 m × 137·8 m	122 m × 137·8 m	122 m × 137·8 m
Block 1 alone	55 m × 59·3 m	55 m × 59·3 m	55 m × 59·3 m

fied engineering disciplines. The semivariogram, a frequently used function in geostatistics, characterises the dependence existing between variables (z values) at different points in space. The value of the semivariogram for a separation distance h is the semivariance, which is the average squared difference in z values between pairs of input sample points separated by h. The semivariance and separation distance at which the semivariogram levels off are known as the sill (C) and range (a). A theoretical semivariogram always starts at 0 (for $h = 0$, $z_{i+h} = z_i$), if there are no measurement errors in the data. If the semivariogram does not level off for large values of separation distance, it indicates that the dataset is non-stationary (Kulatilake & Ghosh, 1988).

However, when the borehole locations are spaced in an irregular pattern over a site, which is common in a typical site exploration strategy, the evaluation of the semivariogram is not as easy as it is for regularly spaced data. The practice in this case calls for the distances and directions to be grouped into classes (Olea, 1999), and for the semivariance to be evaluated considering all the data grouped in each direction or class.

The experimental semivariogram obtained above has to be fitted to the standard analytical semivariogram models, and the parameters of the best fit should be used in further analysis. Clark (1979) provided a number of semivariogram models, and described the process of fitting a model to an empirical semivariogram by a trial-and-error approach. The range of the semivariogram is equivalent to the correlation distance, that is, the distance within which the soil property shows strong correlation. For regularly spaced data the empirical semivariogram is usually determined up to a lag, k, of one fourth or one half of the total number of data points in the database (Journel & Huijbergts, 1978; Clark, 1979), where $k = h/d$ is the normalised separation distance defined as the ratio of the separation distance h to the distance d between two successive points in a database, and which can take only integer values. Moreover, the minimum number of pairs of data at each lag, k, for a reliable estimate of the semivariogram is between 30 and 50 (Journel & Huijbergts, 1978).

In geotechnical engineering practice, data from the routine exploration programme may not be sufficient to quantify the variability of in situ soil properties. In order to predict the unknown values of the founding depth indicators at an unsampled location, a geostatistical-based estimation technique called kriging is commonly used. Kriging is an advanced interpolation procedure based on the assumption that the estimation at any arbitrary point within an objective area can be expressed with linear weighting of all the measured data within the effective domain around the estimation location. Kriging uses the parameters of theoretical functions fitted to a sample semivariogram constructed with either the measured data from the sampled locations or the transformed data, depending on which dataset satisfies the stationarity condition. Recently, Murakami *et al.* (2006) used the kriging technique for land subsidence mapping in the northern Kanto plain of Japan. More details on evaluating the weights assigned to measured data points around the objective location and the prediction methodology are given in Murakami *et al.* (2006). The accuracy of the kriging estimate depends on

(*a*) the number of observations, and the quality of the data at each point
(*b*) the positions of the observations within the deposit – evenly spaced samples achieve better coverage and thus give more information about the deposit than clustered samples do
(*c*) the distance between the observations within the deposit – it is natural to rely more heavily on neighbouring samples, and the prediction accuracy is high in the vicinity of the samples.

Random field modelling

A classical way of describing random functions is through the autocorrelation function $\rho(k)$, which is the coefficient of correlation between values of a random function at a separation distance of $h = kd$. Available methods for estimating the sample autocorrelation functions differ in their statistical properties, such as the degree of bias, sampling variability, ease of use and computational requirements (Akkaya & Vanmarcke, 2003). The methods that are commonly used for this purpose include the method of moments, Bartlett's approach, based on the maximum likelihood principle, and geostatistics. The method of moments is most commonly used to estimate sample correlation functions of soil properties. The spatial correlation of a soil property can be modelled as the sum of a trend component and a residual term (Vanmarcke, 1977)

$$x = t + e \tag{1}$$

where x is the measurement at a given location, t is the trend component and e is the residual (deviation about the trend). The residuals off the trend tend to exhibit spatial correlation. The degree of spatial correlation among the residuals can be expressed through an autocovariance function

$$c(k) = E\left\{[P(Z_i) - t(Z_i)][P(Z_{i+k}) - t(Z_{i+k})]\right\} \tag{2}$$

where $E[.]$ is the expectation operator, $P(Z_i)$ is the value of the soil property at location i, and $t(Z_i)$ is the value of the trend of the soil property at location i. When the dataset does not exhibit a trend, $t(Z_i)$ is the mean value of the data. The normalised form of the autocovariance function is known as the autocorrelation function

$$\rho(k) = \frac{c(k)}{c(0)} \tag{3}$$

where $c(0)$ is the autocovariance function at zero separation distance, which is the variance of the data. It is not possible to evaluate $c(k)$ or $\rho(k)$ with any certainty, but only to estimate them from samples obtained from a population. As a result, the sample autocovariance $c(k)^*$ and the sample autocorrelation $r(k)$ are generally evaluated. The sample autocorrelation function (ACF) is the graph of $r(k)$ for lags $k = 0, 1, 2, \ldots, m$, where m is the maximum number of lags allowed for obtaining reliable estimates. Generally, m is taken as a quarter of the total number of data points in time series analysis of geotechnical data (Box *et al.*, 1994). Beyond this number, the number of pairs contributing to the autocorrelation function diminishes, and unreliable results may be obtained. The sample ACF at lag k, $r(k)$, is generally evaluated using the equation

$$r(k) = \frac{\dfrac{1}{(N-k-1)}\displaystyle\sum_{i=1}^{N-k}\left(X_i - \overline{X}\right)\left(X_{i+k} - \overline{X}\right)}{\dfrac{1}{(N-1)}\displaystyle\sum_{i=1}^{N}\left(X_i - \overline{X}\right)^2} \tag{4}$$

where N is the total number of data points available; X_i and X_{i+k} are the values of the variable at points i and $i+k$ respectively; and $\overline{X}$ is the mean value of the variable.

The autocorrelation characteristics of soil properties can be characterised either by autocorrelation distance or by scale of fluctuation (δ). Analytical models are fitted to the sample autocorrelation functions using regression analysis based on the OLS error approach. Some of the frequently used models and the relation between autocorrelation distance and scale of fluctuation for these models are presented in Jaksa *et al.* (1999). Only positively correlated data need to be considered when fitting a theoretical function, as negative autocorrelation coefficients have no significance in the evaluation of the scale of fluctuation. A small scale of fluctuation, δ, for a dataset implies rapid fluctuations about the mean, and large scales imply slow fluctuations about the mean. Wickremesinghe & Campenella (1993) presented an excellent example. The sleeve friction from a cone penetration test exhibits slow fluctuations around the mean, and is associated with a higher scale of fluctuation, as compared with the rapidly fluctuating cone tip resistance, which exhibits a lower scale of fluctuation. The difference in the fluctuations of the cone tip resistance and sleeve friction is due mainly to the fact that the cone tip resistance is measured at a discrete point at the cone tip, whereas the sleeve friction represents an average value over the length of the friction sleeve.

The autocorrelation characteristics obtained from the measured data alone and those obtained from the combination of the measured data and the kriged data at unsampled locations may not be the same. In this paper the autocorrelation characteristics are analysed with and without kriged data.

RESULTS AND DISCUSSION

Prediction of founding depth indicators at unsampled location

The borehole locations are limited and unevenly spaced over the site under study, as shown in Fig. 2. To achieve the first objective of the study, the founding depth indicators (depths of Grade III, SPT-200 and CDG) are predicted at unsampled locations using the spatial interpolation technique, kriging. The measured data along with the predicted data are used to map the three profiles over blocks 1, 2 and 3 and the whole site. Tables 2 and 3 show the number of measured data and the size of the sampling domain under each category. Relatively fewer measured data are available for the Grade III profile compared with the SPT-200 and CDG profiles. The data refer to the information from the boreholes on the depths to the profile under consideration (Grade III or SPT-200 or CDG).

For regularly spaced boreholes the number of pairs of data at small lags is always greater than that at larger lags, and it is suggested that the maximum lag up to which the semivariance is deemed to be appropriate is $N/4$, where N is the total number of data points (Box *et al.*, 1994). However, for irregularly spaced data the number of pairs of data does not always decrease with increase of lag. Depending on the scatter of the data points, the number of data points at small lags may be smaller than that at larger lags, as observed in the present study. The semivariogram for lags up to $N/4$ as suggested above may not be reliable for irregularly spaced data, as very small numbers of pairs are available at smaller separation distances, and also the number of pairs of data is substantially large for lags greater than $N/4$. Hence it is suggested that the semivariance data corresponding to those lags for which the number of contributing pairs is greater than a particular value (i.e. 30, as suggested in Box *et al.* (1994)) be considered, irrespective of any constraint on the maximum lag. In most of the present analyses, the number of pairs of data corresponding to the first six lags is less than 10. Hence those semivariance data points that result from fewer than 30 pairs are excluded when evaluating the parameters of a theoretical fit to the empirical semivariogram.

The borehole locations are irregularly spaced over the whole site, and the separation distances of all the pairs of data are evaluated. To facilitate division of the measured data into a number of pairs according to the separation distance for evaluating the empirical semivariogram, all the pairs of data are grouped into different classes of 1 m separation interval, and the semivariance is calculated using all the pairs of data categorised into a separation interval. Using the measured values of the founding depth indicators from various borelogs, the semivariance is found to increase continuously with the separation distance, and unrealistic founding depth indicators at unsampled locations are produced. Kulatilake & Ghosh (1988) demonstrated that such a phenomenal increase of semivariance with separation distance could be attributed to a possible trend in the measured data. Accordingly, all the measured sets of data for the depths of Grade III, SPT-200 and top of CDG are verified for a significant trend, and the detrending process (removing low-order polynomials, generally not higher than second degree order) is applied where it is deemed necessary.

Figure 3(a) shows the sample semivariogram of the measured depth of Grade III data obtained from the whole site. It is clearly seen from the figure that the semivariance increases with separation distance without reaching a sill, and produces a range many times greater than the largest separation distance among all the samples in the area under consideration. Hence it is evident from these results that the Grade III data follow a trend. When such a monotonically increasing trend is observed in the empirical semivariance, it should be removed before using it in the evaluation of the semivariogram. A linear trend is identified using the OLS error approach, and the data are detrended accordingly. For the depth of Grade III data from the whole site, the linear trend is

$$z = 298{\cdot}95 - 0{\cdot}15x - 0{\cdot}19y \qquad (5)$$

where x, y and z are the east coordinate, the north coordinate, and the depth of Grade III weathered rock below ground level respectively. Fig. 3(b) shows the sample semivariogram for the linearly detrended data. From this figure it can be seen that the semivariogram increases up to approximately 130 m, and starts diminishing with further increase

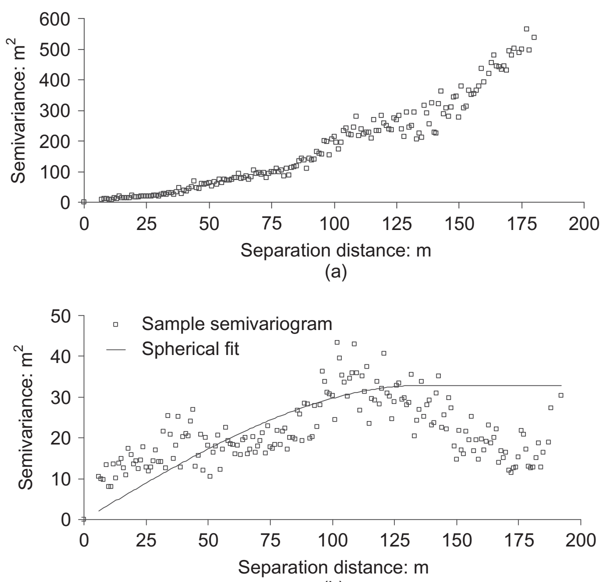

Fig. 3. Comparison of semivariograms for: (a) measured data; (b) linearly detrended data for Grade III from whole site

of separation distance. Several theoretical functions are available to fit experimental semivariogram data (Jaksa *et al.*, 1999), which are shown in Table 4. A theoretical spherical model is used here to fit the sample semivariogram obtained using the linearly detrended data. The parameters of the fitted model, range and sill, are shown in Table 5. Similarly, using the data from blocks 1, 2 and 3 together, and block 1 alone, the observed linear trends are

$$z = 342{\cdot}08 - 0{\cdot}21x - 0{\cdot}17y \quad \text{(blocks 1, 2 and 3 together)} \tag{6}$$

$$z = 207{\cdot}03 - 0{\cdot}10x - 0{\cdot}11y \quad \text{(block 1 alone)} \tag{7}$$

It is decided to predict the founding depth indicators over individual blocks and the whole site at locations spaced 1 m in both directions on plan for mapping all the three profiles. A founding depth indicator at an unsampled location is predicted using the parameters of the theoretical best fit to the sample semivariogram. The theoretical best-fit parameters are used to evaluate the weights to be assigned to all the points around the unsampled location. Fig. 4 shows the profile of the Grade III depth over the whole site using the measured data, as well as the predicted data at unsampled locations.

It is observed that the measured depths of SPT-200 do not follow a significant trend. Hence the measured data are used directly in evaluation of the sample semivariance. The range and sill for this profile are 174 m and 67·4 m^2 respectively. Fig. 5 shows the profile of the depth of SPT-200 for the whole site using both measured and kriged data. Similarly, Fig. 6 shows the profile of the top of the CDG over the whole site.

Error of prediction of founding depth indicators

An effort is made in this study to quantify the range of error in the predicted values of the indicators. Two cases are considered for this purpose. In the first case, a Grade III data point with coordinates 606·96N and 965·53E, shown as A in Fig. 2 within the densely populated location, is neglected, and the depth of Grade III at that location is predicted from kriging using only 173 of the total of 174 data points. The measured depth of Grade III at this point was 36·5 m and the prediction analysis results in a depth of 36·7 m. Hence the error of the prediction in this case is

Table 5. Parameters of semivariogram for different profiles using the data from the whole site

	Grade III	SPT-200	Top of CDG
Range: m	136·3	174	117
Sill: m^2	32·9	67·4	14·1

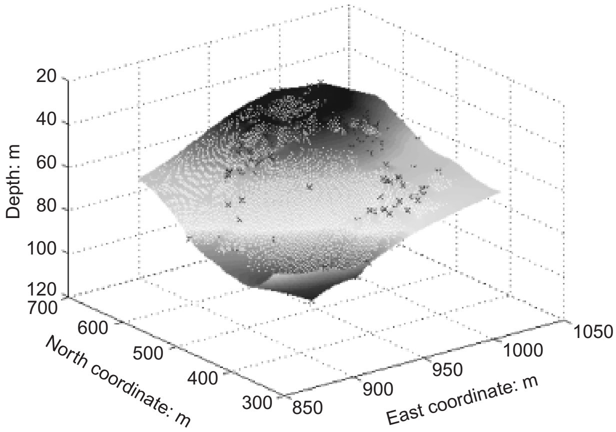

Fig. 4. Profile of depth of Grade III surface over whole site using measured and predicted data

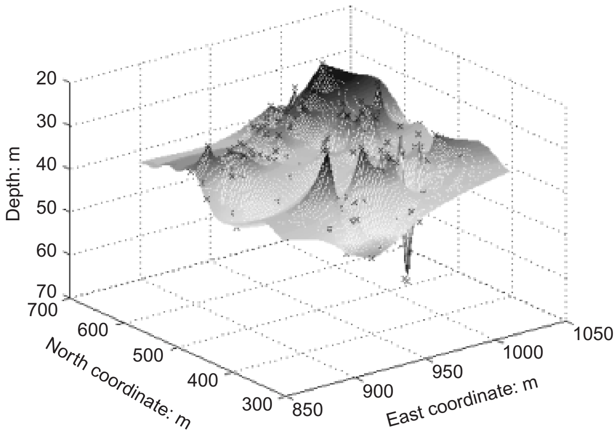

Fig. 5. Profile of depth of SPT-200 surface over whole site using measured and predicted data

Table 4. Typical semivariogram fitting models

Model	Mathematical expression
Exponential	$\gamma(h) = C\left[1 - \exp\left(\frac{-h}{a}\right)\right]$
Squared exponential	$\gamma(h) = C\left\{1 - \exp\left[-\left(\frac{h}{a}\right)^2\right]\right\}$
Spherical	$\gamma(h) = \begin{cases} C\left[1{\cdot}5\left(\frac{h}{a}\right) - \frac{1}{2}\left(\frac{h}{a}\right)^3\right] & \text{for } \lvert h\rvert < a \\ C & \text{for } \lvert h\rvert \geqslant a \end{cases}$
Cubic	$\gamma(h) = \begin{cases} C\left(\frac{7h^2}{a^2} - \frac{35h^3}{4a^3} + \frac{7h^5}{2a^5} - \frac{3h^7}{4a^7}\right) & \text{for } \lvert h\rvert \leqslant a \\ C & \text{for } \lvert h\rvert > a \end{cases}$

h, C and a are the separation distance, sill and range of the theoretical fit; $\gamma(h)$ is the semivariance at separation distance h.

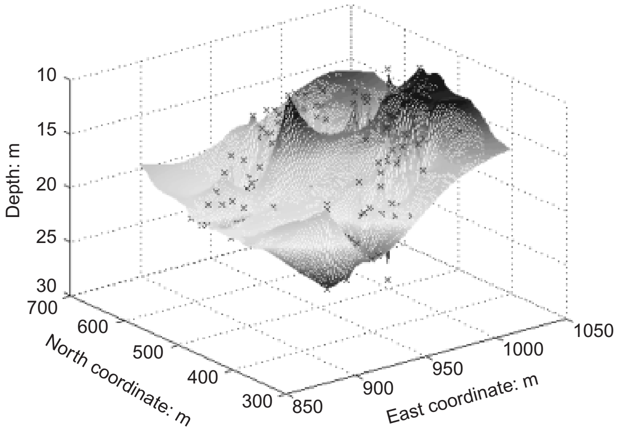

Fig. 6. Profile of top of CDG surface over whole site using measured and predicted data

0·2 m. In the second case, a remote data point (coordinates 482·43N, 911·15E, and shown as B in Fig. 2), which is surrounded by very few data points, is neglected from the 174 data points. The measured depth of Grade III of this data point is 79·1 m, and the depth obtained from the prediction model is 79 m. The error of the prediction in this case is 0·1 m. The same procedure described above is adopted to evaluate the error of prediction at those locations in the case of SPT-200 and top of CDG surfaces, and the results are shown in Table 6. It may be argued that the error of prediction at any unsampled location may range between 0·1 m and 0·2 m for Grade III, between 0·1 m and 0·2 m for SPT-200, and between 0·1 m and 0·3 m for CDG profiles. However, further studies are warranted to understand the range of error of prediction at all the 174 data points, and to minimise the level of uncertainty in the estimated parameters of kriging, which are beyond the scope of the present work.

Spatial autocorrelation characteristics of weathered soils

As previously outlined, kriging produces weighted average estimates at unsampled locations, and it is argued that the spatial correlation characteristics of the measured values and those estimated using kriging would be quite different, as, in the process of weighted averaging, the original correlation structure of the soil would be altered. Hence, for estimating the representative spatial correlation characteristics at the study site, it was decided to use the measured data of the founding depth indicators alone, and the estimated data at unsampled locations are kept aside completely. However, to show the differences in the estimated spatial correlation characteristics with and without consideration of interpolated data, results obtained using the combined dataset of measured and interpolated data are also presented.

Results using the measured data only

Fenton (2000) demonstrated that if trend details at other sites are not present, or are different from the present site, then the removal of the trend from the studied site results in statistics that are unconservative. In particular, estimated scales of fluctuation and variance values will be smaller than those that would result if the site details were treated as part of the overall randomness of the site. Since the objective of obtaining spatial variability characteristics of founding depth indicators at the study site is to help the engineer for nearby sites or sites of similar geological origins to develop an effective and efficient planning of future site investigation, the measured data are used in the analysis without the removal of any trend. Fig. 7 shows the variation of the sample autocorrelation coefficients with separation distance for the measured Grade III data for the whole site. A theoretical best fit based on the method of OLS is chosen for quantifying the spatial variability. A triangular function (Jaksa *et al.*, 1999) is observed to fit the sample autocorrelation data best, and subsequently the scale of fluctuation for these data is estimated as 84·7 m. Similarly, the measured data of the SPT-200 and CDG profiles over the whole site produce autocorrelation coefficients as shown in Figs 8 and 9, and the scales of fluctuation of these profiles are obtained as 18·5 m and 8·6 m respectively. These results are shown in Table 7. When the data from the whole site are considered, the Grade III profile, which is categorised as moderately decomposed rock, exhibits a scale of fluctuation of 84·7 m, which is around 4·5 and 10 times larger than that obtained for the SPT-200 and CDG profiles respectively.

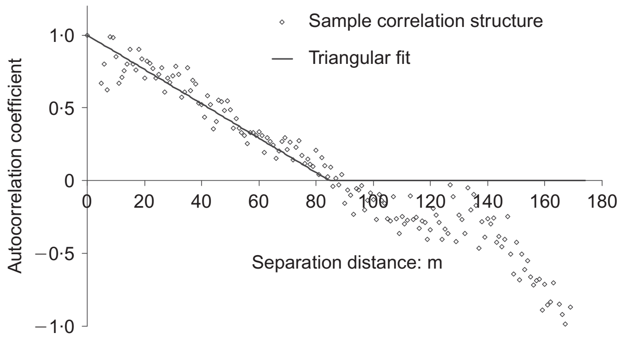

Fig. 7. Sample autocorrelation function for Grade III surface using only measured data within whole site

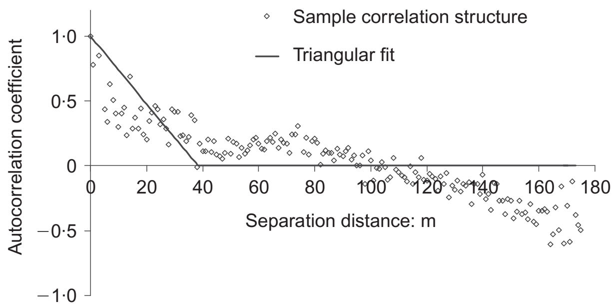

Fig. 8. Sample autocorrelation function for depth of SPT-200 profile using only measured data within whole site

Table 6. Error of prediction of founding depth indicators

Property	Location A			Location B		
	Grade III	SPT-200	CDG	Grade III	SPT-200	CDG
Measured: m	36·5	34·5	19·4	79·1	45·5	18·9
Predicted: m	36·7	34·3	19·1	79·0	45·4	19·0
Error: m	0·2	−0·2	−0·3	−0·1	−0·1	0·1

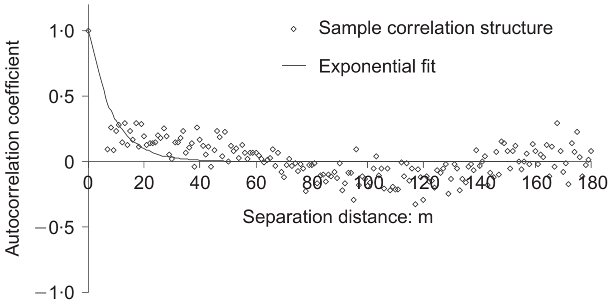

Fig. 9. Sample autocorrelation function for CDG profile using only measured data within whole site

Table 7. Scale of fluctuation (m) for all three profiles using only measured data

	Grade III	SPT-200	Top of CDG
Data for the whole site	84·7	18·5	8·6
Data for blocks 1, 2 and 3	30·2	15·2	6·0
Data for block 1	20·3	9·7	6·0

The larger scale of fluctuation for the Grade III depth profile implies that the fluctuations of the depth of Grade III weathered rock at individual borehole locations about the mean profile are very small, and the average mean crossover distance of Grade III weathered rock is large. Here, the crossover distance is defined as the distance between two consecutive depths at which the fluctuating soil property crosses the trend function. In other words, it can be said that on average, when the data from the whole site are considered, the depth of the Grade III profile is strongly correlated to a distance of 84·7 m.

Results using combined dataset

Figure 10 shows the sample autocorrelation function evaluated using the combined data, utilising both measured and predicted data, for the depth of the Grade III surface over the whole site. A squared exponential function (Jaksa *et al.*, 1999), which is shown with a solid line, has been identified as giving a good fit to the sample autocorrelation data. Table 8 summarises the scales of fluctuation obtained for the squared exponential function using the combined dataset. Similarly, the scales of fluctuation for SPT-200 and CDG profiles are also obtained using the combined data obtained from the whole site, and are also shown in Table 8.

By comparing the results obtained from the measured data alone and the combined data comprising the measured data from site investigation and the kriged data at unsampled locations, it is revealed that these two datasets produce quite

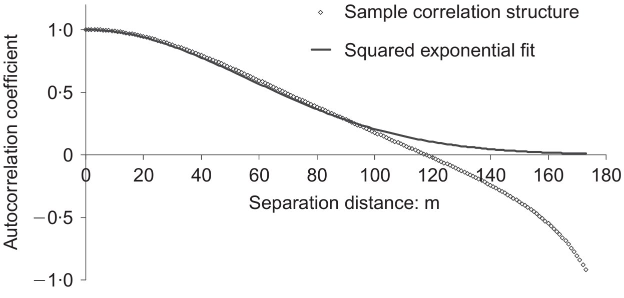

Fig. 10. Sample autocorrelation function for Grade III surface using combined data within whole site

Table 8. Scale of fluctuation (m) for all three profiles using combined data

	Grade III	SPT-200	Top of CDG
Data for the whole site	141·1	44·6	59·2
Data for blocks 1, 2 and 3	78·4	43·1	23·9
Data for block 1	27·1	32·8	26·9

different scale of fluctuation values, with smaller scales of fluctuation associated with the former dataset (measured data alone). Moreover, the Grade III profile exhibits the largest scale of fluctuation of all the three profiles for both datasets. In the case when only the measured data are considered, the scale of fluctuation of the SPT-200 profile is larger than that of the CDG profile. Nonetheless, the CDG profile produces a larger scale of fluctuation than the SPT-200 profile, when the combined dataset is used.

Effect of the size of the sampling domain

Analysis is carried out to identify how the size of the sampling domain affects the autocorrelation characteristics of the founding depth indicators. Previous studies revealed that the spatial characteristics of soil parameters change with the size of the sampling domain, with a larger sampling domain producing a larger scale of fluctuation (DeGroot & Baecher, 1993). Cafaro & Cherubini (2002) also noticed that the scale of fluctuation increases with sample spacing. In summary, most of the previous studies have been confined to a regularly spaced dataset. However, in this section, the measured data, which are irregularly spread over the study domain, are used to study the effect of the size of the sampling domain on the spatial correlation characteristics of the founding depth indicators.

Figures 11(a) and 11(b) show the autocorrelation coefficients for the Grade III profile using the data from blocks 1, 2 and 3 together and from block 1 alone. The scales of fluctuation for these two datasets are given in Table 7. It can be seen from this table that the scale of fluctuation increases with increase in the size of the sampling domain for this profile.

Figures 12(a) and 12(b) show the autocorrelation coefficients for the SPT-200 profile using the data from blocks 1, 2 and 3 together and from block 1 alone. Similarly, the autocorrelation coefficients for the top of the CDG profiles are shown in Figs 13(a) and 13(b) using the data from blocks 1, 2 and 3 together and from block 1 alone respectively. The same trend of increased scale of fluctuation with increasing size of sampling domain is also observed for the SPT-200 and CDG profiles, except for the scale of fluctuation obtained for the CDG profile using the data from block 1 alone. The estimated scales of fluctuation of the top of the CDG profiles using data from blocks 1, 2 and 3 and from block 1 alone are the same. The latter may be a biased estimate, caused by the limited number of pairs of data at small separation distances. These results are presented in Table 7.

Larger scales of fluctuation are obtained for all the three founding depth indicators when the data within the whole site are considered. In the case of the Grade III profile, the scale of fluctuation obtained using the data from the whole site is almost four times larger than that obtained using the data from block 1 alone. In the case of the SPT-200 profile, this ratio is around two. However, the observed increase in the scale of fluctuation with increased size of the sampling domain is marginal (40%) for the top of the CDG profile.

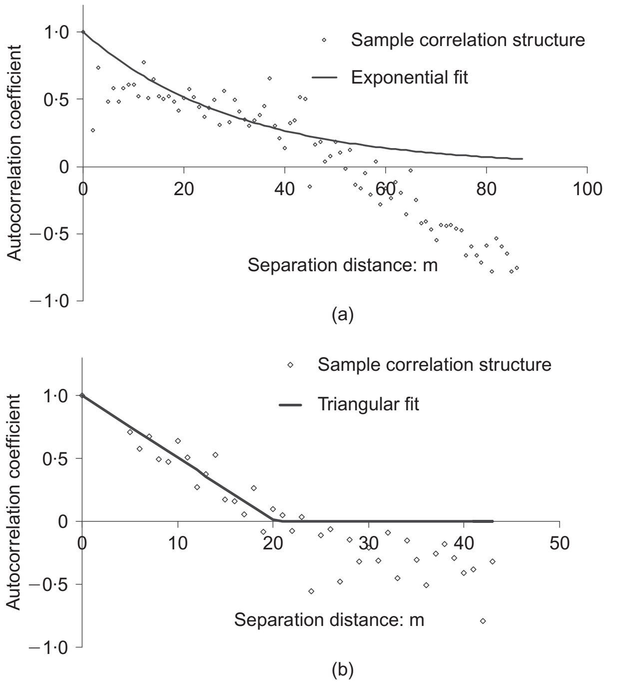

Fig. 11. Sample autocorrelation function for Grade III surface: (a) using measured data obtained from blocks 1, 2 and 3; (b) using measured data from block 1 alone

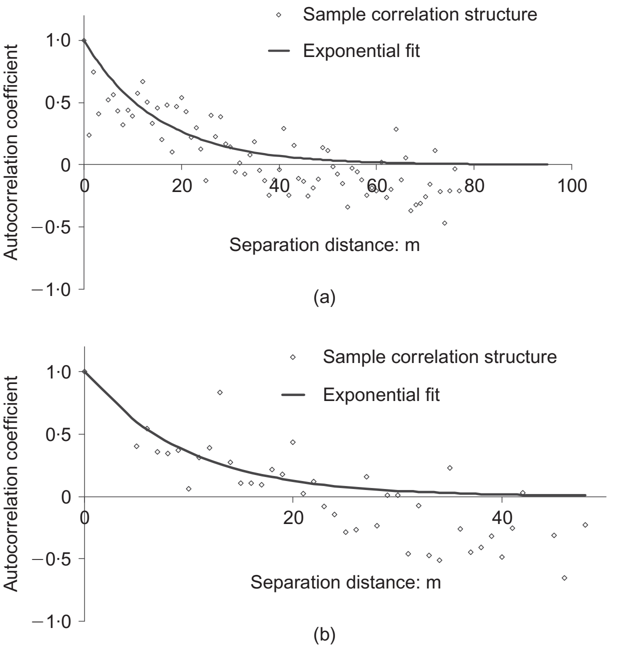

Fig. 12. Sample autocorrelation function for SPT-200 surface: (a) using measured data obtained from blocks 1, 2 and 3; (b) using measured data from block 1 alone

From the site investigation results it is found that, among the three profiles, the top of the CDG profile was found to be at shallow depths, followed by the SPT-200 and Grade III profiles. In terms of the spatial variability of these three profiles over the site, the depth of the Grade III surface is found to exhibit the largest scale of fluctuation, followed by the depth of the SPT-200 surface and the top of the CDG, for all sizes of sampling domain. Hence it can be concluded that the deepest profile (Grade III) has the largest scale of fluctuation, and the shallowest profile (CDG) has the smallest scale of fluctuation. This phenomenon of decreased scale of fluctuation associated with increasing weathering grade

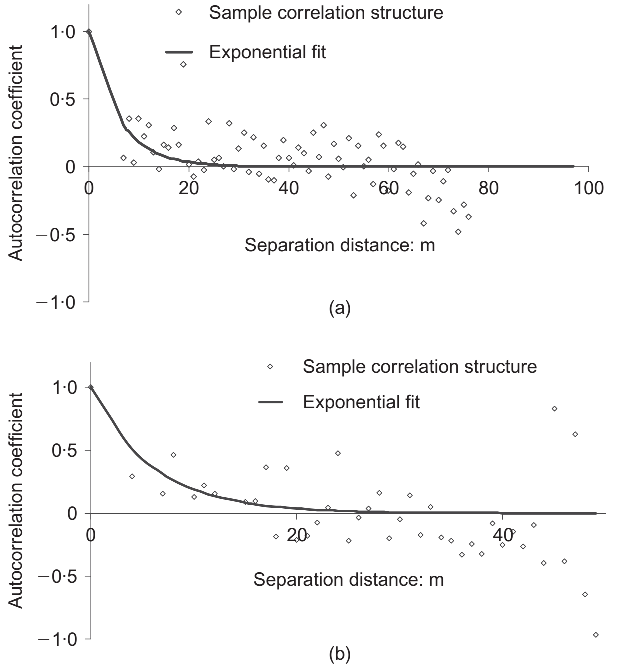

Fig. 13. Sample autocorrelation function for top of CDG surface: (a) using measured data obtained from blocks 1, 2 and 3; (b) using measured data from block 1 alone

may be attributed to the weathering intensity, whereby a strong correlation exists for unweathered or moderately weathered rock profiles.

When the measured data from blocks 1, 2 and 3 are considered, the Grade III profile exhibits a scale of fluctuation of 30·2 m, which is around two and five times larger than those obtained for the SPT-200 and CDG profiles respectively. These ratios obtained using measured data from block 1 are 2·1 and 3·4 respectively.

The results obtained from the analyses clearly show that the scale of fluctuation of a soil parameter varies not only from site to site, depending on the site geological conditions, stress history and other parameters, but also at a particular residual-soil site with the size of the sampling domain.

From the results of the analyses for this site, three different magnitudes of scale of fluctuation are obtained for each of the founding depth indicators, based on the size of sampling domain. However, if the whole site needs to be represented by a unique value of the scale of fluctuation, the largest scale of fluctuation corresponding to the largest exploration area is preferred, which produces a conservative estimate of the variance, as suggested by Fenton (2000).

To identify the effect of using the combined data, comprising the measured data and the predicted data from kriging, on the estimated scales of fluctuation, results are summarised in Table 8. Comparing the scales of fluctuation obtained from these two datasets (i.e. the measured data alone and the measured data combined with the predicted data), it is observed that the latter data produce significantly higher scales of fluctuation for all the profiles and all sizes of sampling domain.

Implication for current geotechnical practice

The findings in this paper have implications for current geotechnical investigation procurement strategy. It is worth considering the following points while building an accurate ground model, which may include such information as the level of Grade III weathered rock, and the top of CDG or SPT-200 profiles for design using sparse field data. Practitioners should

(*a*) consider the use of data derived from nearby sites or sites of similar geological materials subjected to similar geological process to build a preliminary ground model for a new site – this preliminary ground model can be used to guide new investigations at the new site
(*b*) ensure that no fault is present at the new site and the nearby sites, as this may make predictions less reliable
(*c*) combine the data from the new site with existing predictions and related data from nearby sites to refine the ground model.

CONCLUSIONS

The spatial correlation characteristics of founding depth indicators are studied in this paper using the data obtained from in situ investigation in weathered rock. The depth of the Grade III weathered rock is an important indicator used in Hong Kong design practice to evaluate the preliminary founding depth of bored piles. Similarly, the depth of the SPT-200 is used as a reference founding depth for driven piles. The top of the CDG is also used to assist in preliminary designs for founding depth of pile foundations. The following are some significant conclusions arrived from the present study.

(*a*) The scale of fluctuation is observed to decrease with increasing weathering grade. The Grade III profile exhibits larger scales of fluctuation than the SPT-200 and CDG profiles. This confirms that, when faults are not present, a stronger correlation exists within unweathered or moderately weathered rock profiles at great depths than in soil profiles found at relatively shallow depths.
(*b*) The scale of fluctuation increases with the size of the sampling domain. The results obtained from the analyses reveal that a larger scale of fluctuation is obtained when using the data from the whole site, than when using the data either from blocks 1, 2 and 3 together, or from block 1 alone.
(*c*) To map the profiles over the site, the kriging technique is adopted. A monotonically increasing trend is observed in semivariograms constructed with measured Grade III data, which suggests that the dataset follows a linear trend. Hence a linear trend based on the OLS approach is removed from the measured data. However, no significant trend is observed in the SPT-200 and CDG profiles.
(*d*) The error in the prediction of the founding depth indicators at two extreme locations varies in the range 0·1–0·3 m, depending on the position of the unsampled location with respect to those of the measured data.
(*e*) The scales of fluctuation obtained using the combined data (i.e. the measured data from site investigation and the predicted data from kriging) are significantly larger than those obtained using the measured data alone.

ACKNOWLEDGEMENTS

The work reported in this paper is substantially supported by the Research Grants Council of the Hong Kong Special Administrative Region (Project No. 622308).

REFERENCES

Akkaya, A. & Vanmarcke, E. H. (2003). Estimation of spatial correlation of soil parameters based on data from the Texas A&M University National Geotechnical Experimentation Site (NGES). In *Probabilistic Site Characterization at the NGES* (eds E. VanMarcke and G. A. Fenton), GSP 121, pp. 29–40. Reston, VA: ASCE.

Box, G. E. P., Jenkins, G. M. & Reinsel, G. C. (1994). *Time series analysis: Forecasting and control*, 3rd edn. Englewood Cliffs, NJ: Prentice Hall.

Brooker, P. I. (1991). *A geostatistical primer*. Singapore: World Scientific.

Cafaro, F. & Cherubini, C. (2002). Large sample spacing in evaluation of vertical strength variability of clayey soil. *J. Geotech. Geoenviron. Engng ASCE* **128**, No. 7, 558–568.

Campanella, R. G., Wickremesinghe, D. S. & Robertson, P. K. (1987). Statistical treatment of cone penetrometers test data. *Proc. 5th Int. Conf. on Applications of Statistics and Probability in Soil and Structural Engng, Vancouver*, 1011–1019.

Clark, I. (1979). *Practical geostatistics*, London: Applied Science.

DeGroot, D. J. (1996). Analyzing spatial variability of in-situ soil properties. In *Uncertainty in the geologic environment: From theory to practice* (eds C. D. Shackelford, P. P. Nelson and M. J. S. Roth), GSP 58, pp. 210–238. Reston, VA: ASCE.

DeGroot, D. J. & Baecher, G. B. (1993). Estimating autocovariance of in-situ soil properties. *J. Geotech. Engng, ASCE* **119**, No. 1, 147–166.

Durgin, P. B. (1977). Landslides and the weathering of granitic rocks. *Rev. Engng Geol*. **3**, 127–131.

Fenton, G. A. (1999). Random field modeling of CPT data, *J. Geotech. Geoenviron. Engng ASCE* **125**, No. 6, 486–498.

Fenton, G. A. (2000). Closure to 'Random field modeling of CPT data'. *J. Geotech. Geoenviron. Engng ASCE* **126**, No. 12, 1214–1216.

Fletcher, C. J. N. (2004). *Geology of site investigation boreholes from Hong Kong*. Hong Kong: Association of Geotechnical and Geoenvironmental Specialists (Hong Kong).

GEO (2000a). *Guide to site investigation*, Geoguide 2. Geotechnical Engineering Office, The Government of the Hong Kong Special Administrative Region.

GEO (2000b). *Guide to rock and soil descriptions*, Geoguide 3. Geotechnical Engineering Office, The Government of the Hong Kong Special Administrative Region.

GEO (2006). *Foundation design and construction*, Publication No. 1. Geotechnical Engineering Office, The Government of the Hong Kong Special Administrative Region.

Jaksa, M. B., Kaggwa, W. S. & Brooker, P. I. (1999). Experimental evaluation of the scale of fluctuation of a stiff clay. *Proc. 8th Int. Conf. on the Application of Statistics and Probability, Sydney* **1**, 415–422.

Journel, A. G. & Huijbergts, C. J. (1978). *Mining geostatistics*. London: Academic Press.

Kulatilake, P. H. S. W. (1989). Probabilistic potentiometric surface mapping. *J. Geotech. Engng ASCE* **115**, No. 11, 1569–1587.

Kulatilake, P. H. S. W. & Ghosh, A. (1988). An investigation into accuracy of spatial variation estimation using static cone penetration data. *Proc. 1st Int. Symp. on Penetration Testing, Orlando, FL*, 815–821.

Kulhawy, F. H., Birgisson, B. & Grigoriu, M. D. (1992). *Reliability-based foundation design for transmission line structures: Transformation models for* in situ *tests*, Report EL-5507(4). Palo Alto, CA: Electric Power Research Institute.

Liu, C.-N. & Chen, C.-H. (2006). Mapping liquefaction potential considering spatial correlations of CPT measurements. *J. Geotech. Geoenviron. Engng ASCE* **132**, No. 9, 1178–1187.

Lumb, P. (1974). *Application of statistics in soil mechanics: New horizons*. New York: American Elsevier.

Murakami, S., Yasuhara, K., Suzuki, K. & Komine, H. (2006). Reliable land subsidence mapping using a spatial interpolation procedure based on geostatistics. *Soils Found*. **46**, No. 2, 123–134.

Olea, R. A. (1999). *Geostatistics for engineers and earth scientists*. Boston, MA: Kluwer Academic.

Vanmarcke, E. H. (1977). Probabilistic modeling of soil profiles. *J. Geotech. Engng. Div. ASCE* **103**, No. GT11, 1227–1246.

Wickremesinghe, D. & Campenella, R. G. (1993). Scale of fluctuation as a descriptor of soil variability. In *Probabilistic methods in geotechnical engineering* (eds K. S. Li and S.-C. R. Lo), pp. 233–240. Rotterdam: Balkema.

Zhang, L. M. & Dasaka, S. M. (2010). Uncertainties in geologic profiles versus variability in pile founding depth. *J. Geotech. Geoenviron. Engng ASCE* **136**, No. 11, 1475–1488.